Single-Cell RNA-Seq Reveals Adventitial Fibroblast Alterations during Mouse Atherosclerosis

Lauren E. Fries, Allen Chung, Hyun K. Chang, Timothy Yuan, Robert C. Bauer

Authors, Affiliation, ORCID ID:

- Lauren E. Fries - Cardiometabolic Genomics Program, Division of Cardiology, Department of Medicine, Columbia University, New York, NY, USA; 0000-0003-3148-440X
- Allen Chung - Cardiometabolic Genomics Program, Division of Cardiology, Department of Medicine, Columbia University, New York, NY, USA; 0000-0002-2494-9179
- Hyun-Kyung Chang - Cardiometabolic Genomics Program, Division of Cardiology, Department of Medicine, Columbia University, New York, NY, USA; 0000-0002-3490-7597
- Timothy Yuan - Cardiometabolic Genomics Program, Division of Cardiology, Department of Medicine, Columbia University, New York, NY, USA; 0009-0006-6215-2212
- Robert C. Bauer - Cardiometabolic Genomics Program, Division of Cardiology, Department of Medicine, Columbia University, New York, NY, USA; 0000-0001-9752-9645

***Correspondence to**

Robert C. Bauer, Ph.D.

630 W. 168th Street, PS10-401,

New York, New York 10032, USA.

E-mail: rcb36@columbia.edu

Abbreviations:

- Atherosclerotic cardiovascular disease (ASCVD)
- ECM → Extracellular matrix
- CAD → Coronary artery disease
- CVD → Cardiovascular disease
- WD → Western diet
- GWAS → Genome-wide association study
- LDL → Low-density lipoprotein

Abstract

Atherosclerotic cardiovascular disease (ASCVD) is the leading cause of mortality in the western world, despite great successes with lipid lowering therapies. This alarming trend highlights the need for novel lipid-independent therapeutic strategies for the treatment of ASCVD. Unbiased genome-wide association studies (GWAS) have identified numerous genes associated with ASCVD that have led to efficacious therapies, indicating that the pathways and genes identified are essential for providing insight into the cellular mechanism behind ASCVD. ASCVD GWAS suggest that vascular cells mediate ASCVD progression, and in vivo studies suggest that some of these genes may function in the adventitia of the vasculature. To further explore a role for adventitial cell types in atherosclerosis, we performed a time course western diet (WD) feeding experiment in *Ldlr*$^{-/-}$ mice, completing single cell RNA-sequencing (scRNA-seq) of the aortic adventitia to determine cellular and transcriptomic changes in this region during disease progression. We found a surprising diversity of adventitial fibroblasts that demonstrate population size changes and gene expression alterations over the course of atherogenesis. These populations included previously highlighted fibroblast populations expressing *Anxa3, Cd55, Lox,* and *Cpe*. We next cross-referenced our murine scRNA-seq with published ASCVD GWAS dataset and identified *SERPINH1* as a differentially expressed GWAS gene in adventitial fibroblasts during atherosclerosis which is also linked to ASCVD. Further *in vitro* studies showed that knockdown of *SERPINH1* in human adventitial fibroblasts reduced migration and altered expression of fibroblast subcluster marker genes. Our data suggests that reduced *SERPINH1* expression in adventitial fibroblasts during atherosclerosis progression is altering the function and identity of adventitial fibroblasts, contributing to disease progression. Collectively, these findings highlight the changing nature of adventitial fibroblasts during atherogenesis, and, specifically, the potential role of *SERPINH1* in mediating these processes.

Introduction

Atherosclerotic cardiovascular disease (ASCVD) is the leading cause of death in the United States[1]. The infiltration of low-density lipoprotein (LDL) particles into the vascular intima initiates atherosclerosis, and therefore therapeutic strategies have historically focused on reducing circulating LDL levels. Despite the widespread use of these LDL-lowering therapies, residual mortality from ASCVD remains high. Thus, there is strong interest in developing novel non-LDL-lowering therapies[2]. Unbiased genome-wide association studies (GWAS) have successfully identified novel genes and biological processes associated with ASCVD that may represent novel therapeutic avenues. GWAS have routinely identified genes involved in LDL metabolism, but also genes involved in inflammation and vascular cell biology. We know that LDL reduction reduces ASCVD incidence, and recent clinical trials have shown that targeting inflammation to treat ASCVD is also therapeutically efficacious[3]. Thus, pathways identified by GWAS can provide insight into the progression of ASCVD and generate potential new treatment strategies.

As the vasculature is the site at which atherosclerosis develops, it is perhaps not surprising that GWAS have repeatedly identified genes that appear to predominantly function in vascular cell types. However, given the cellular complexity of the vasculature, it is unclear which genes function in which cell types and in which portion of the vessel wall. Arteries consist of three primary layers: the intima, which is the innermost layer and comprises predominantly a monolayer of endothelial cells; the media, a middle layer external to the intima and primarily composed of smooth muscle cells; and the adventitia, the outermost layer consisting mainly of fibroblasts but also known to contain various cell types, including smooth muscle cells, T cells, B cells, macrophages, and endothelial cells. Many recent studies have primarily explored the role of intimal and medial cells in atherosclerosis, but the adventitia has received far less attention. Intriguingly, multiple ASCVD-associated GWAS genes, including *ADAMTS7 and TCF21* [4,5], are expressed in the adventitia in both mouse and human atherosclerosis tissue. Furthermore, in vivo mouse studies have shown that fibroblasts can migrate from the adventitia into the neointima after vascular balloon injury[6]. These findings support a more substantial role of the adventitia in atherogenesis than previously appreciated, and suggest that interrogation of the role of the adventitia during atherogenesis may highlight novel therapeutic pathways.

In this study, we sought to leverage single-cell RNA sequencing (scRNA-seq) to characterize the transcriptome of the vascular adventitia during atherosclerosis development in the low-density lipoprotein receptor knockout (*Ldlr* KO) mouse model of atherosclerosis. Our results identified dynamic changes in adventitial fibroblasts during atherogenesis. We show that the expression of *Serpinh1*, an ASCVD GWAS gene, changes in fibroblasts during atherogenesis in both humans and mice. Finally, *in vitro* studies indicate that *SERPINH1* promotes fibroblast migration and proliferation. These findings link human ASCVD GWAS data to the adventitia, highlighting an essential role for the adventitia in atherosclerosis and identifying a potential novel disease mechanism.

Results

scRNA-seq of the adventitia of atherosclerotic *Ldlr*$^{-/-}$ mice

To elucidate the effect of atherosclerosis progression on the adventitia, *Ldlr*$^{-/-}$ mice were fed a western-type diet for 0, 9, or 16 weeks. The aorta was dissected at the specified time points,

and the adventitia was mechanically isolated from the aorta and dissociated for single-cell RNA sequencing, with six mice used at each timepoint (Fig. 1A). After Illumina sequencing and pre-processing steps, including quality control, and UMAP clustering, we employed previously established cell lineage markers to identify and label six major cell types: T cells, B cells, macrophages, fibroblasts, smooth muscle cells, and endothelial cells (Fig. 1B). Notably, the initiation of western diet (WD) feeding caused a trend towards a contraction of fibroblasts and an expansion of immune cells from 0 to 9 weeks of WD feeding (Fig. 1C). However, the proportion of each cell population showed no statistically significant changes throughout the progression of the experiment (Fig. 1C). Overall, fibroblasts make up the largest proportion of cells (Fig. 1C). B cells were the only population with no significant changes in gene expression during the time course. Examining gene expression profiles in the adventitia revealed changes encompassing CAD-associated GWAS genes such as *Abca1* during the timecourse of WD feeding, both overall and within specific cell types (Fig. 1D, Supp Table3). Gene set enrichment analysis (GSEA) unveiled a shift in immune and ECM-associated genes, in agreement with the observed reduction in fibroblasts and expansion of immune cells during atherosclerosis progression (Fig. 1E). Specifically, ECM-related processes were downregulated while immune-related processes were upregulated (Fig. 1F). Collectively, this data underscores significant changes, both at the genetic and cellular levels, that occur in the adventitia during the formation of atherosclerotic plaques, suggesting that not only are the intima and media altered, but the adventitia as well.

Subsetting Fibroblasts Identifies Four Distinct and Biologically Relevant Fibroblast Populations

Given that fibroblasts make up the majority of adventitial cells, and prior literature suggesting their involvement in atherogenesis, we next subclustered and re-analyzed the fibroblast scRNA-seq data to better understand the function of adventitial fibroblasts in atherosclerosis. We identified four unique fibroblast clusters that we have labeled Fibroblast1-4 (Fig. 2A). A subset of Fibroblast1 and Fibroblast2 displayed an *Acta2* signature, indicating that these cell types are likely myofibroblasts[7]. Fibroblast3, and to a lesser extent, Fibroblast4, demonstrated elevated expression of the stem-like marker *Ly6a* [7,8] (Fig. 2B). Additionally, Fibroblast3 expressed *Cd55* and *Anxa3* (Fig. 2B), genes that have been previously used to mark fibroblast subclusters in other reports [9]. Fibroblast1 expressed *Lox* and *Cpe*, two other previously identified markers of specific fibroblast clusters[9]. We next performed pseudotime analysis to identify any transitions between fibroblast clusters. This analysis corroborated our fibroblast classifications, as we found a transition from stem cell-like fibroblasts in Fibroblast3 towards a more differentiated cell state in Fibroblast1 and Fibroblast2 (Fig. 2C). Throughout atherosclerosis progression, Fibroblast1 and Fibroblast3 trended towards expansion, whereas Fibroblast2 contracted in a statistically significant manner, consistent with transdifferentiation of the latter into the former. Fibroblast4 trended towards contraction as well, suggesting that the Fibroblast2 and Fibroblast4 subtypes potentially play a role in the cellular response to plaque formation (Fig. 2D). We next determined the differential gene expression amongst all four clusters between week 0 of WD feeding and weeks 9 and 16, revealing a list of 2575 significantly altered genes (Fig. 2E). Some of the identified genes are previously associated with ASCVD, such as *Apoe*, *Col4a1*, *Lpl*, *Abca1*, and *Ldlr* (Supp. Table6), but the majority of these genes are known to alter ASCVD incidence through functions in lipid metabolism. Alternatively, other identified genes have limited previous data connecting them with cardiovascular disorders, such as *Hnrnpa3* and *Serpinh1* (Supp. Table6). Consistent with the broader analysis of all cells,

GSEA of fibroblast DE genes highlighted substantial changes in immune and ECM-associated genes during plaque development (Fig. 2F). These findings underscore the diverse populations of adventitial fibroblasts and shed light on the significant genetic and cellular alterations during atherosclerosis.

Identification of *SERPINH1* as an adventitial fibroblast gene of interest

Given that ASCVD GWAS genes have been previously shown to be expressed in adventitial cells in atherosclerosis, we next sought to identify genes previously identified through ASCVD GWAS[10] that were differentially expressed in our dataset. We built a pipeline starting with CAD GWAS genes found by Aragam et al and refined this list by filtering against our scRNA-seq differentially expressed genes in the fibroblast cluster (Fig. 3A). The GWAS study we used uncovered 716 unique genes at a 1% false discovery rate. We subsequently screened these genes against those differentially expressed between time points in fibroblasts in our adventitia dataset, resulting in 82 common genes. Gene ontology (GO) enrichment was initially performed on this list of 82 cross-referenced genes. GO revealed that these differentially expressed genes primarily involved ECM remodeling (Fig. 3B), highlighting the role of the adventitia in ECM deposition.

The list of these 82 genes was further refined by removing genes with less than 1 TPM expression in the human artery GTEx data set, leaving 75 genes. Next, only genes with more than 1.25 fold change in W0 vs either W9 or W16 were kept, reducing the number to 48 genes. We next removed any genes previously associated with lipid pathways as determined by GWAS, leaving 40 genes[11]. Around one-third of the differentially expressed genes were downregulated from WD W0 to W9 and W16, while the other two-thirds were upregulated during the progression of atherosclerosis (Fig. 3C). Finally, only genes that are highly expressed in fibroblasts and expressed in less than two other cell types were kept, resulting in a final list of five genes.

The final five differentially expressed novel atherosclerosis-associated genes are *Cxcl12, Col6a3, Col4a1, Serpinh1,* and *Loxl1* (Fig. 3D). *Serpinh1* stood out as a gene of interest due to its high expression levels across all fibroblast subsets. Expression of *Serpinh1* varies across time and fibroblast subcluster. Over all fibroblasts, *Serpinh1* expression is statistically reduced during atherosclerosis progression, though Fibroblast1 and Fibroblast3 show higher expression levels compared to the other two fibroblast clusters (Fig. 3E, Supp. Table6). Although smooth muscle and endothelial cells display some *Serpinh1* expression, this expression does not change during atherosclerosis in those cell types as determined by differential gene expression analysis. The WD *Ldlr*$^{-/-}$ mouse model indicates that *Serpinh1* is an adventitial fibroblast gene that is reduced during atherosclerosis, but to determine the clinical relevance we aimed to corroborate these results in humans.

HSP47 is a protein of interest in human atherosclerosis.

We next interrogated available human evidence supporting a role for *SERPINH1* in ASCVD. The lead CAD GWAS SNP (rs584961) is a synonymous coding variant in exon 2 of *SERPINH1,* consistent with *SERPINH1* being the causal gene at this GWAS locus[12] (Fig. 4A). Additionally, cultured fibroblast eQTL analysis indicates decreased expression of *SERPINH1* with the risk allele, which correlates to increased risk of coronary artery disease (Fig. 4B). Specifically, for SNP rs584961, the G risk allele corresponds to a reduction of expression, suggesting that a

decrease in *SERPINH1* is atherogenic [10]. These data are consistent with our observation that fibroblast *Serpinh1* expression decreases over the course of atherogenesis, suggesting that the GWAS association between ASCVD and *SERPINH1* may be explained in part by the function of this gene in fibroblasts.

We next set out to determine if the cell type expression patterns we observed in our mouse scRNA-seq data were reproducible in humans. To investigate if human fibroblasts also exhibit altered expression of *SERPINH1* in atherosclerosis, we extracted and reanalyzed a previously published scRNA-seq dataset from three patients undergoing carotid endarterectomy [13]. The study included two "samples:" one is labeled as "proximal," and was obtained from a full artery thickness, excluding the adventitia, while the second sample is denoted as "plaque," and was procured from the atherosclerotic core. We performed subset analysis of the cell clusters in this data and identified two distinct fibroblast populations, two smooth muscle populations, and two immune-like populations (Fig. 4C). Consistent with our observations in the Ldlr KO mouse model of atherosclerosis, *SERPINH1* expression was predominately in fibroblasts (Fig. 4D). Notably, within the plaque sample, a downregulation of *SERPINH1* expression was observed between "proximal" healthy tissue and "plaque" data (Fig. 4E). We do acknowledge that these data were generated from tissue samples lacking human adventitial fibroblasts, as the adventitia was excluded from sample collection. However, there is currently no publicly available scRNA-seq dataset from atherosclerotic tissue that includes adventitial fibroblasts. Overall, the reduced expression of *Serpinh1* during murine atherosclerosis mirrors the reduction in *SERPINH1* expression seen in plaque versus proximal samples, consistent with the notion that fibroblast *SERPINH1* may play a more significant role in atherogenesis than previously recognized.

SERPINH1 **Knockdown Decreases Fibroblast Migration and Proliferation**

Finally, we next sought to test in vitro if altering *SERPINH1* expression levels would alter adventitial fibroblast function. To that end, we knocked down *SERPINH1* expression via siRNA in primary human aortic adventitial fibroblasts (hAoFs) (Fig. 5A). We assessed the migratory defects of the knockdown with a scratch assay. Knockdown of *SERPINH1* resulted in a 20% reduction in hAoFs migration over the course of 8 hours as compared to cells receiving a non-targeting control siRNA (Fig. 5B & 5C). Conversely, there was no change in hAoF proliferation between the siRNA knockdown and the control, consistent with any chances in migration being due to movement of the cells and not differences in proliferative capacity (Fig. 5D). Lastly, we performed qPCR to assess any changes in the expression of the previously identified fibroblast subcluster markers due to *SERPINH1* knockdown. We observed increases in both *ANXA3* and *LOX* expression levels when *SERPINH1* was knocked down (Fig. 5E), mirroring the increase in both of the cell types these genes are markers of in later atherosclerosis timepoints in our mouse data. Collectively, these results demonstrate that *SERPINH1* regulates adventitial fibroblast function *in vitro* in a manner consistent with *in vivo* observations made during mouse atherosclerosis.

Discussion

Here, we present the first comprehensive single-cell atlas of adventitial cells over the course of atherogenesis in hyperlipidemic *Ldlr*-/- mice, expanding upon prior studies that focused on the *Apoe*$^{-/-}$ background or the non-leukocyte populations within the adventitia of Ldlr-/-mice at static

timepoints[7,8]. Our findings reveal that fibroblasts constitute the vast majority of cells within the adventitia. Over the course of atherosclerosis progression, we observe a contraction of the fibroblast population and an expansion of immune cells. These cellular changes are accompanied by alterations in ECM gene expression, primarily in fibroblasts, during atherogenesis. Furthermore, we identify four different fibroblast subclusters, one of which significantly contracts during atherogenesis. Finally, we highlight *SERPINH1* as a ASCVD GWAS gene that likely plays a role in adventitial fibroblast function during atherosclerosis.

The role of adventitial fibroblasts in atherogenesis remains largely unexplored[8]. Unlike macrophages, which have traditionally been categorized as either pro or anti-inflammatory, the functional subsets of fibroblasts in atherosclerosis are not well-defined. Moreover, while atherosclerosis has typically been viewed as an inside-out inflammatory process, emerging evidence suggests an outside-in model, where inflammation originates in the adventitia, and the effects perpetuate to the intima[14]. Supporting this, a prior study demonstrated that transplanted adventitial fibroblasts migrate to the intima following balloon injury[6]. Furthermore, multiple genes identified by ASCVD GWAS studies also demonstrate adventitial expression in models of atherosclerosis and vascular injury[4]. Understanding the role of adventitial fibroblasts and their subtypes in atherosclerosis is crucial, as these cells are likely contributing to plaque formation and progression.

In our study, we highlight the diversity of adventitial fibroblasts over the course of atherogenesis in mice. We identified four distinct adventitial fibroblast populations, two of which (Fibroblast1 and Fibroblast2) express Acta2, a marker of myofibroblasts. Fibroblast3 and Fibroblast4 both exhibited elevated expression of the stem-like marker *Ly6a*, indicating a more transitional state [7,8]. Indeed, pseudotime analysis of our data aligns with these observations, suggesting transitions between myofibroblasts and stem cell-like subclusters. Notably, we observed a significant contraction of the Fibroblast2 cluster over the course of atherosclerosis, suggesting that loss of this cell type coincides with the progression of atherosclerosis. Our fibroblast clusters somewhat align with previously described subclusters in the literature. For example, Fibroblast3 expressed *Cd55* and *Anxa3*, and Fibroblast1 expressed *Lox* and *Cpe*, each found to be identifying markers of specific fibroblast trajectories in prior studies[9]. Notably, a recent study identified four distinct fibroblast subsets present in atherosclerotic plaques, suggesting some may contribute to plaque development [7]. Further experimentation with these adventitial fibroblast subtypes will be required to delineate the distinct subsets and their potential functions to better understand their individual contributions to atherosclerosis.

In this study, we also cross-referenced our Murine scRNA-seq with published human ASCVD GWAS datasets in hopes of identifying human genes with translational potential. We identified *SERPINH1* as a differentially expressed gene in adventitial fibroblasts during atherosclerosis that also has been linked to ASCVD in human GWAS. HSP47, the protein encoded by *SERPINH1*, acts as a collagen-specific chaperone essential for proper collagen folding[15]. HSP47 is highly evolutionarily conserved, indicating its crucial role in normal biological function. Reduced HSP47 levels have been linked to impaired cell migration and proliferation, resulting in ineffective scar formation[16,17]. Combined GWAS and eQTL analysis suggests that lower expression of *SERPINH1* correlates with increased CAD risk (Fig. 4B). Interestingly, patients with asymptomatic atherosclerosis exhibited increased expression of *SERPINH1*[18], highlighting a potential role for *SERPINH1* in plaque stability. Our scRNA-seq matches these findings, as we

found reduced *Serpinh1* expression in adventitial fibroblasts as atherosclerosis progressed. Finally, we found in vitro that knockdown of *SERPINH1* in human adventitial fibroblasts reduced fibroblast migration and altered expression of fibroblast subcluster marker genes (*ANXA3*, *LOX*). Taken together, these human genetic and in vitro data suggest that reduced *SERPINH1* expression during atherosclerosis progression is altering the function and identity of adventitial fibroblasts. How exactly these changes in migration and gene expression promote atherosclerosis is the focus of ongoing studies.

In conclusion, our scRNA-seq analysis underscores the biological and functional diversity of adventitial fibroblasts during atherosclerosis. We highlight *SERPINH1* as a ASCVD GWAS gene that shows reduced expression in both mouse and human atherosclerosis, suggestive of an anti-atherogenic effect. We show in vitro that knockdown of *SERPINH1* in cultured human adventitial fibroblasts impairs their migration and correlates with expression of fibroblast markers increased during atherosclerosis progression, suggesting that *SERPINH1* plays a critical role in fibroblast function and cluster identity. Further studies are needed in rodent models to explore the role of *SERPINH1* and other CAD GWAS genes in adventitial cells during atherosclerosis. Our findings underscore the current interest in the role of adventitial fibroblasts in atherosclerosis and, specifically, the role of the chaperone *SERPINH1*.

Author Contributions

LEF completed all analyses of data and completed *in vitro* work. AC, HKC acquired the single RNA-sequencing mouse data. AC, TY conducted experiments and acquired data. RCB oversaw the design, execution, management, and funding of all studies. LF, AC, and RCB wrote the manuscript, which all authors approved before submission.

Data availability statement:

All sequencing data will be available at a GEO accession number GSExxxx. All R scripts used for data analysis will be added to a github and publicly available.

Acknowledgements:

The Genotype-Tissue Expression (GTEx) Project was supported by the Common Fund of the Office of the Director of the National Institutes of Health, and by NCI, NHGRI, NHLBI, NIDA, NIMH, and NINDS. The data used for the analyses described in this manuscript were obtained from: the GTEx Portal on 12/15/2023 and dbGaP accession number phs000424.v8.p2.

LEF and TY were supported by NIH Graduate Training in Nutrition grant 5T32DK007647. AC was supported by an American Heart Association Predoctoral Fellowship (909206). RCB was supported for this work by NIH grants R01HL141745 and R01DK134026, and by the Katz Cardiovascular Research Award from the Division of Cardiology at Columbia University.

Methods:

Animal studies

The Institutional Animal Care and Use Committee of Columbia University approved all animal experiments under protocol AAAZ4473. *Ldlr*-/- (stock No. 002207) mice were purchased from

the Jackson Laboratory and maintained at Columbia. At 8-10 weeks of age, mice were initiated on a WD (Research Diets, D12079Bi) for 9 or 16 weeks.

Preparation of mouse aortic adventitia for scRNA-seq

Mice were deeply sedated with isoflurane and euthanized by cervical dislocation. The mice were immediately perfused with ice-cold DPBS. The aorta was sharply dissected from the ascending aorta to the bifurcation at the common iliac artery. The aorta was digested in 1 mg/mL of Collagenase A (Roche, 11088793001) in F12:DMEM (Cytiva, SH30023.01) containing 0.2% BSA (Sigma-Aldrich, A9647) at 37℃ to allow for the removal of the adventitia. After 5 minutes, the aorta was moved into DPBS, and the outer adventitia was peeled off. The adventitia layer from 3 mice was pooled and subsequently digested in a cocktail containing 2mg/mL of Collagenase A, 0.05 mg/mL of Elastase (Worthington, LS006365), and 60U/mL of DNase (Worthington Biochemical, LS006331) in F12:DMEM containing 0.2% BSA for 30 minutes at 37℃. The cells were subsequently passed through a 70uM cell strainer and spun down at 300 x g for 5 minutes. The cells were resuspended in F12: DMEM containing 0.2% BSA and 1mg/ml DNase stained with 1:10,000 DAPI and 1:1000 Draq5 (BioLegend, 424101), and live cells were sorted. All scRNA-seq experiments were performed at the JP Sulzberger Genome Center at Columbia University. Samples were prepared using 10x Genomics Chromium Cell 3' Reagent Kits according to the manufacturer's instructions. 5000 cells were inputted with the goal of 100M reads per sample. Sequencing libraries were prepared according to the user manual and then sequenced on Illumina sequencer. FASTQ files were processed through cell ranger.

Analysis of mouse scRNA-seq data

Quality control and data pre-processing

During filtering we excluded cells with < 100 features, UMI count < 500, number of genes < 200, log10GenesperUMI < 0.8, mitochondrial ratio >0.1, any genes expressed in 5 or fewer cells or with zero counts from further analyses. We formed clusters using the top principal components for the shared nearest neighbor (SNN) analysis and a resolution of 0.8. To identify cell types we found differentially expressed genes between the clusters with "FindAllMarkers" function. We identified six broad cell types, including B cells, T cells, fibroblasts, smooth muscle cells, and endothelial cells, of which each cluster was assigned to and merged, the differentially expressed. Fibroblasts were subclustered and reprocessed to obtain 4 distinct clusters at a resolution of 0.22 after two sets of two clusters were combined due to minimal differences in conserved genes. We identified differentially expressed genes between timepoints using the R package 'Nebula'. Gene ontology (GO) enrichment analysis is useful for understanding biological processes that are enriched based on a set of genes. We performed GO enrichment analysis using the 'clusterProfiler' R package. We performed this analysis on the differentially expressed genes between the WD time points across all clusters as well as in fibroblasts subset specifically. We provide visualization of the results with the dotplot function.

Analysis of human scRNA-seq data

Quality control and data pre-processing

Single cell RNA-sequencing samples were obtained from the Gene Expression Omnibus (GEO, GSE159677) [13]. All patients presented with severe carotid plaque formation, which required carotid endarterectomy. Near full thickness (except adventitia) sections of artery and plaque were recovered from three patients from the atherosclerotic core, based on the surgeon's determination of area of largest plaque burden. Patient-matched proximal adjacent portions of

carotid artery tissue were used as the control. The aggregate filtered feature-barcode matrix of the processed single-cell data was pre-processed using the R package 'Seurat' for quality control, normalization, dimensionality reduction, and clustering. We excluded cells expressing less than X or greater than y UMIs / genes, and cells with >z% mitochondrial counts from further analyses. Samples were normalized using SCTransform in Seurat, integration was completed with Seurat's FindIntegrationAnchors function, and dimensionality reduction was performed with standard Seurat processing pipelines. We formed clusters using the top x principal components (PC1 to PCx) for the shared nearest neighbor (SNN) analysis and a resolution of x. To identify cell types we found differentially expressed genes between the clusters with "FindAllMarkers" function. We identified seven clusters, including Immune.1 and Immune.2, Fibroblast.1, Fibroblast.2, SmoothMuscle.1, and SmoothMuscle.2. We used the 'Nebula' R package to identify differentially expressed genes between the proximal and plaque samples and enrichR to determine gene set enrichment features. We used locus zoom to creature the LocusZoom plot [12].

Cell Culture

Human aortic adventitial fibroblasts were purchased from Lonza (Lonza, CC-7014) and cultured in the Stromal Cell Growth Basal Medium containing Stromal Cell Growth Medium SingleQuots Supplements and Growth Factors (Lonza, CC-3205). Only cells between passages 3-7 were used for experiments. Cells were routinely tested for mycoplasma contamination.

siRNA knockdown

All siRNAs were purchased from Integrated DNA Technologies (Integrated DNA Technologies, hs.Ri.SERPINH1.13). Human fibroblasts were seeded on a 12-well plate and transfection was performed using RNAiMAX. siRNAs were transfected at a concentration of 10nM end concentration, and knockdown or further assays were assessed 48 hours post-transfection.

qRT-PCR

RNA from whole cell lysates was extracted using the Directzol Miniprep Kit (Zymo). The cDNA was subsequently synthesized using High-Capacity cDNA Reverse Transcription Kit (Applied Biosystems, 4368813) according to the manufacturer's instructions. Quantitative PCR was performed using Taqman probes on the QuantStudio 7 Flex Real-Time PCR System. Analysis was performed using the ΔΔCT method with normalization against the housekeeping gene Gapdh. n=4 pooled samples of 3 wells each per condition collected after the completion of migration assay, two-tailed unpaired t-test was completed to analyze differences in gene expression between conditions. **** $P<0.0001$, *** $P<0.001$, ** $P<0.01$, ns $P>0.05$.

Proliferation Assay

Cellular proliferation was assessed with the CellTiter 96 AQueous One Solution Cell Proliferation solution (Promega, G3582) according to manufacturers' instructions. In brief, fibroblasts were seeded in a 96-well plate at 5,000 cells/well. The CellTiter reagent was diluted in culture media, and cells were incubated for 2 hours at 37℃ in a humidified incubator. The absorbance was subsequently measured at 490nm. n=8 biological samples per condition and two-tailed unpaired t-test was completed to analyze differences in proliferative activity between conditions. **** $P<0.0001$, *** $P<0.001$, ** $P<0.01$, ns $P>0.05$.

Migration assay

Cellular migration was assessed using the Culture-Insert 2 Well 24 (Ibidi, 80242). Cells were seeded at 20,000 cells/well (one half of insert) 24 hours before migration was assessed, at which point images were obtained using a Nikon Ti-S Automated Inverted Microscope at 10X magnification. Image processing was performed using ImageJ using Wound Healing Size Tool macro on manual mode [19]. n=24 biological samples (wells) per condition, completed over two separate dates, and two-tailed unpaired t-test was completed to analyze differences in migration between conditions. **** P<0.0001, *** P<0.001, ** P<0.01, ns P>0.05.

References:

1. Tsao, C. W. *et al.* Heart Disease and Stroke Statistics—2023 Update: A Report From the American Heart Association. *Circulation* **147**, e93–e621 (2023).
2. Libby, P. The changing landscape of atherosclerosis. *Nature* **592**, 524–533 (2021).
3. Alfaddagh, A. *et al.* Inflammation and cardiovascular disease: From mechanisms to therapeutics. *Am. J. Prev. Cardiol.* **4**, 100130 (2020).
4. Bauer, R. C. *et al.* Knockout of Adamts7, a Novel Coronary Artery Disease Locus in Humans, Reduces Atherosclerosis in Mice. *Circulation* **131**, 1202–1213 (2015).
5. Nurnberg, S. T. *et al.* Coronary Artery Disease Associated Transcription Factor TCF21 Regulates Smooth Muscle Precursor Cells That Contribute to the Fibrous Cap. *PLOS Genet.* **11**, e1005155 (2015).
6. Si, Y. *et al.* Protein kinase C-delta mediates adventitial cell migration through regulation of monocyte chemoattractant protein-1 expression in a rat angioplasty model. *Arterioscler. Thromb. Vasc. Biol.* **32**, 943–954 (2012).
7. Tillie, R. J. H. A., van Kuijk, K. & Sluimer, J. C. Fibroblasts in atherosclerosis: heterogeneous and plastic participants. *Curr. Opin. Lipidol.* **31**, 273–278 (2020).
8. Gu, W. *et al.* Adventitial Cell Atlas of wt (Wild Type) and ApoE (Apolipoprotein E)-Deficient Mice Defined by Single-Cell RNA Sequencing. *Arterioscler. Thromb. Vasc. Biol.* **39**, 1055–1071 (2019).
9. van Kuijk, K. *et al.* Human and murine fibroblast single-cell transcriptomics reveals fibroblast clusters are differentially affected by ageing and serum cholesterol. *Cardiovasc. Res.* **119**,

1509–1523 (2023).

10. Aragam, K. G. *et al.* Discovery and systematic characterization of risk variants and genes for coronary artery disease in over a million participants. *Nat. Genet.* **54**, 1803–1815 (2022).
11. Graham, S. E. *et al.* The power of genetic diversity in genome-wide association studies of lipids. *Nature* **600**, 675–679 (2021).
12. Boughton, A. P. *et al.* LocusZoom.js: interactive and embeddable visualization of genetic association study results. *Bioinformatics* **37**, 3017–3018 (2021).
13. Alsaigh, T., Evans, D., Frankel, D. & Torkamani, A. Decoding the transcriptome of calcified atherosclerotic plaque at single-cell resolution. *Commun. Biol.* **5**, 1–17 (2022).
14. Kuret, T., Sodin-Šemrl, S., Kuret, T. & Sodin-Šemrl, S. The Role of Fibroblasts in Atherosclerosis Progression. in *Fibroblasts - Advances in Inflammation, Autoimmunity and Cancer* (IntechOpen, 2021). doi:10.5772/intechopen.98546.
15. Ito, S. & Nagata, K. Roles of the endoplasmic reticulum–resident, collagen-specific molecular chaperone Hsp47 in vertebrate cells and human disease. *J. Biol. Chem.* **294**, 2133–2141 (2019).
16. YAMAMOTO, N. *et al.* Tumor-suppressive microRNA-29a inhibits cancer cell migration and invasion via targeting HSP47 in cervical squamous cell carcinoma. *Int. J. Oncol.* **43**, 1855–1863 (2013).
17. Khalil, H. *et al.* Cell-specific ablation of Hsp47 defines the collagen-producing cells in the injured heart. *JCI Insight* **4**, e128722.
18. Theofilatos, K. *et al.* Proteomic Atlas of Atherosclerosis: The Contribution of Proteoglycans to Sex Differences, Plaque Phenotypes, and Outcomes. *Circ. Res.* **133**, 542–558 (2023).
19. Suarez-Arnedo, A. *et al.* An image J plugin for the high throughput image analysis of in vitro scratch wound healing assays. *PLoS ONE* **15**, e0232565 (2020).

Figure 1

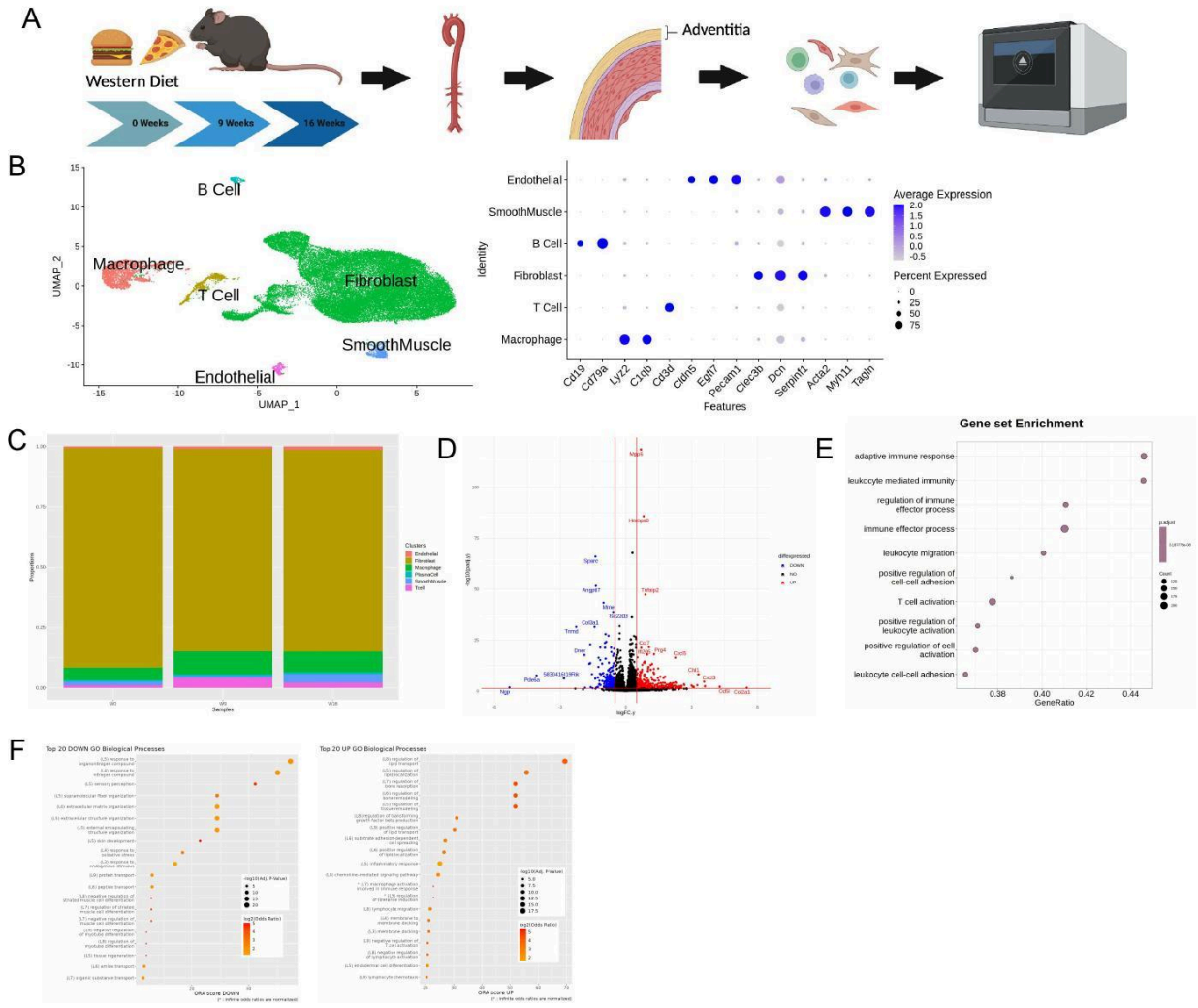

Fig. 1: Adventitial cells during atherosclerosis progression. (A) Schematic of experimental design. Created with Biorender.com (B) UMAP visualization of clustering single-cell clustering reveals six major cell types and top differential expressed genes to aid in cell type identification, n=2 mice per each WD time point. (C) Distribution of each cell type across WD feeding. (D) Volcano plot of differentially expressed genes common between WD week 0 vs WD week 9 and WD week 16. log2FC values are on the x-axis and the y-axis shows the difference between proportions. The left side of the y-axis represents a decrease and the right side represents an increase in expression. (E) Gene set enrichment of W0 vs. W9 and W0 vs. W16. (F) Gene Ontology scoring of the top 20 up and down-regulated biological processes.

Figure 2

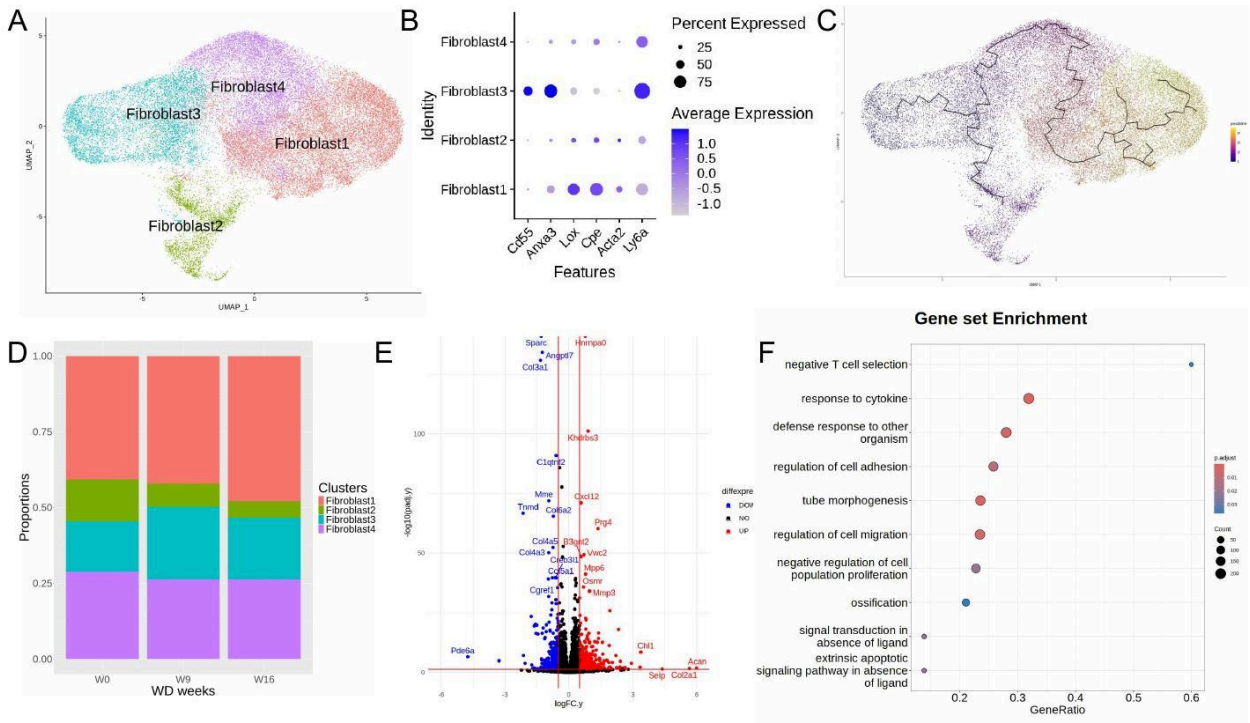

Fig. 2: Diversity of adventitial fibroblasts and changes during atherogenesis. (A) Subsetting of fibroblasts uncovers four populations. (B) Expression patterns of distinguishing gene features. (C) Pseudotime analysis of fibroblast subsets. (D) Distribution of each fibroblast subset across WD feeding (E) Top differentially expressed genes of W0 vs. W9 and W0 vs. W16, specifically in fibroblasts. (F) Gene set enrichment of W0 vs. W9 and W0 vs. W16 in fibroblasts.

Figure 3

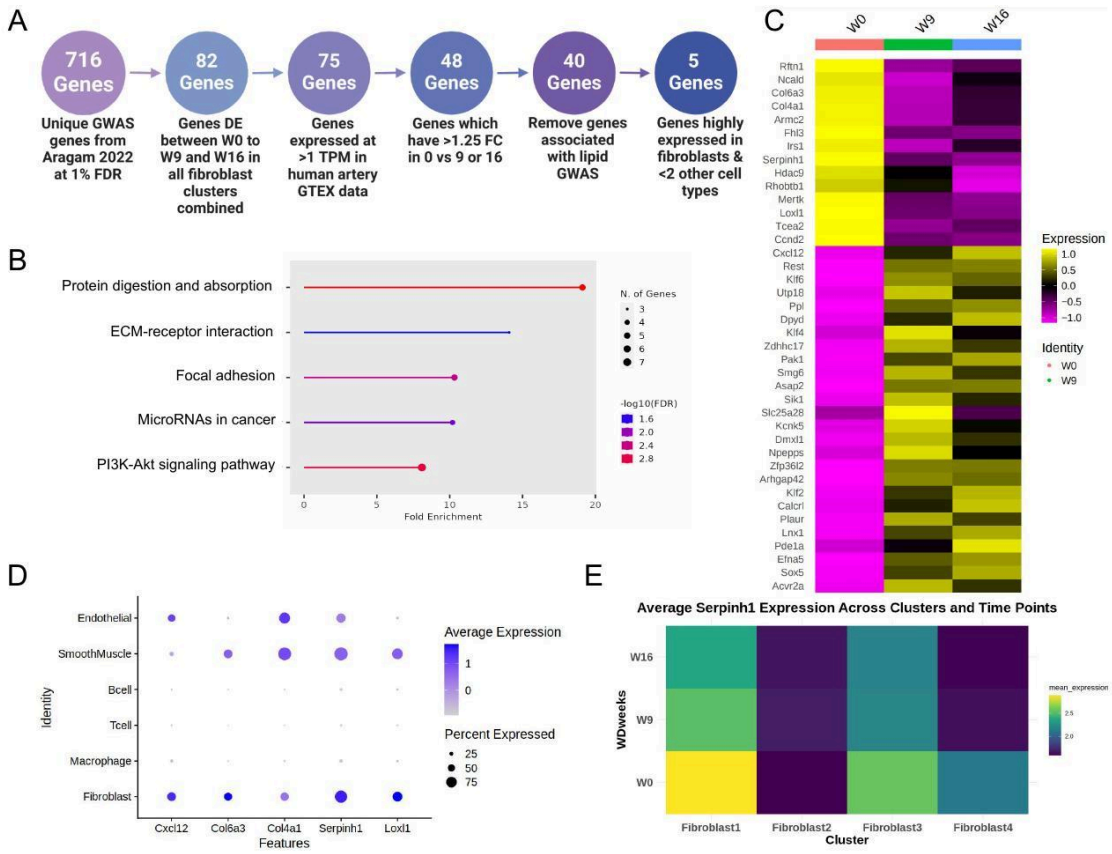

Fig. 3: CAD GWAS gene cross analysis with expression changes during atherosclerosis in mice. (A) Computational pipeline for cross-referencing CAD GWAS hits and differentially expressed adventitial fibroblast scRNA-seq identified genes. (B) Gene ontology analysis of the 82 matched cross-referenced genes between CAD GWAS and scRNA-seq. (C) Differentially expressed CAD GWAS genes in adventitial fibroblasts across WD feeding. (D) The six identified adventitial fibroblast CAD GWAS genes of interest. (E) Expression of *Serpinh1* within fibroblast subsets across WD feeding.

Figure 4

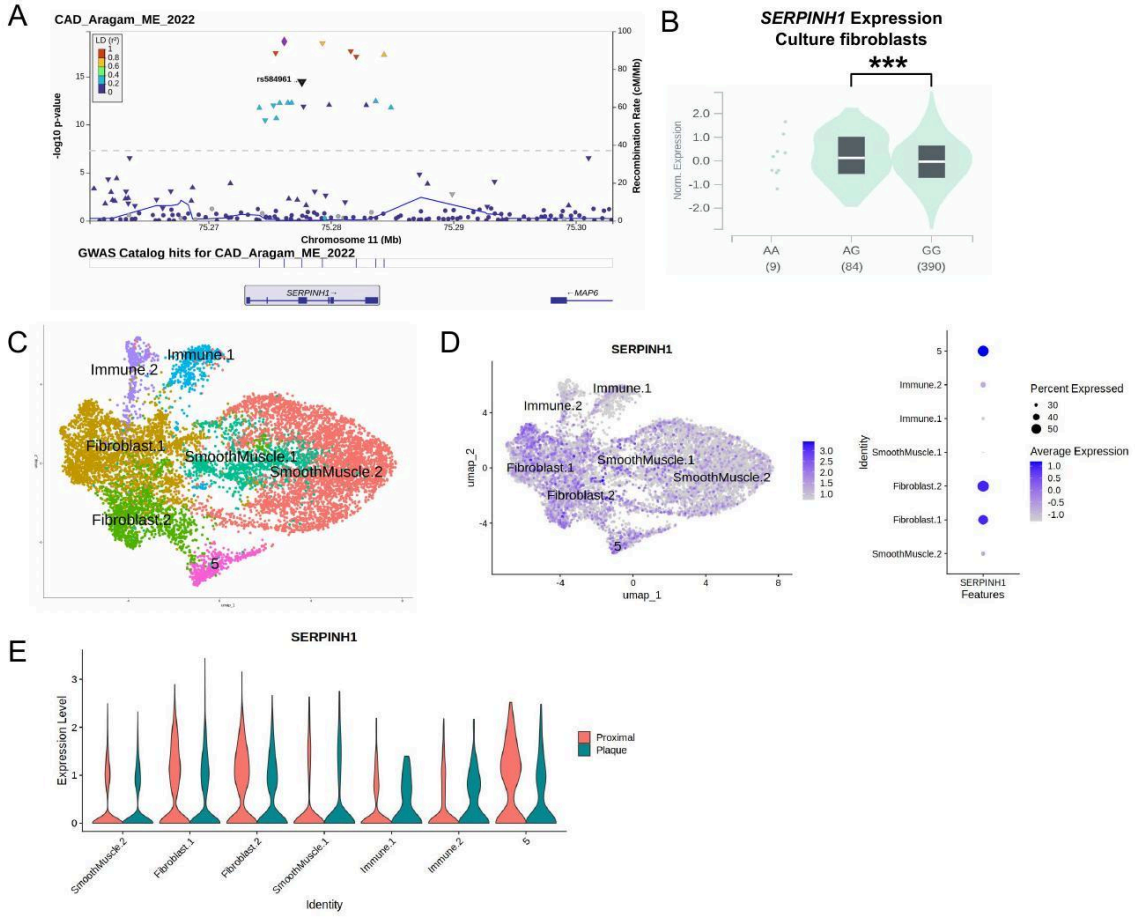

Fig. 4: Examination of *SERPINH1* in humans during atherosclerosis. (A) Locus zoom plot of *SERPINH1*. (B) eQTL of *SERPINH1* SNP derived from GTEx (pvalue=9.84e-18). (C) Basic clustering identities of the joint analysis between proximal and plaque samples of human carotid arteries. (D) Expression of *SERPINH1* across different cell types. (E) Differential *SERPINH1* expression between the two plaque states.

Figure 5

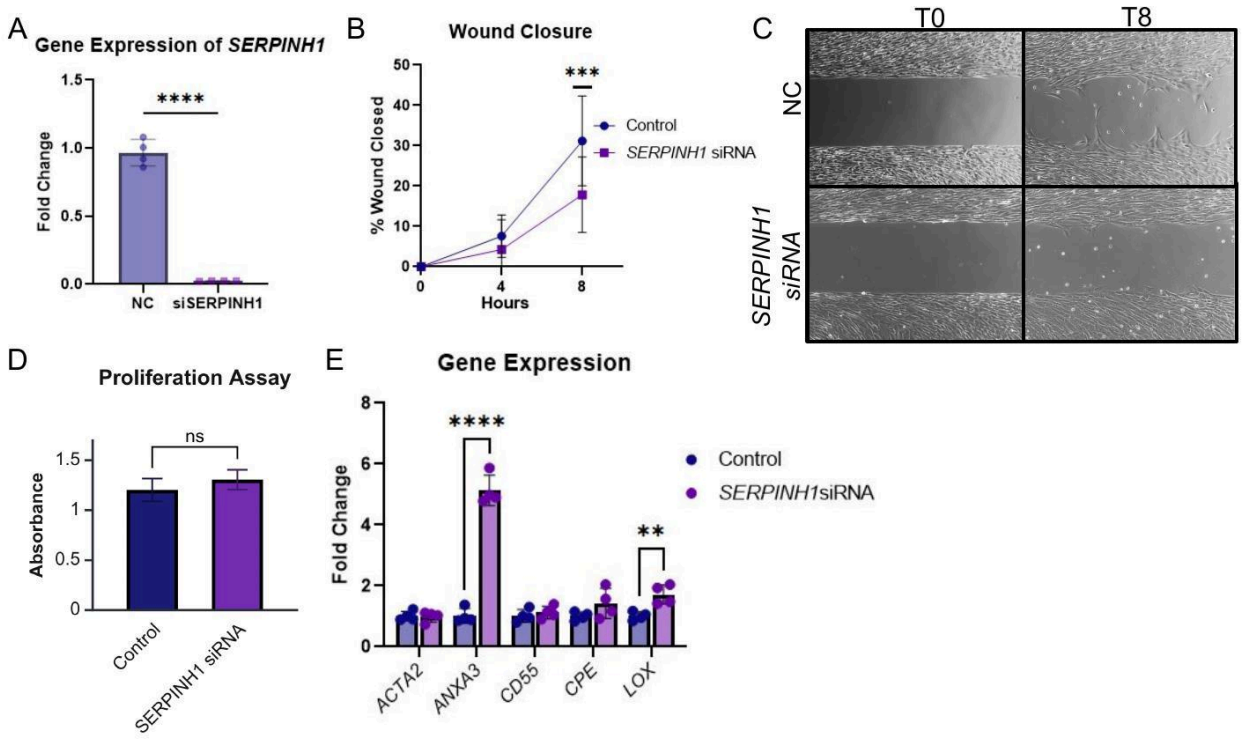

Fig. 5: Knockdown of *SERPINH1* in human adventitial fibroblasts. (A) Confirmation of *SERPINH1* siRNA knockdown. (B) Quantification of migration assay. (C) Representative image of migration assay. (D) MTT proliferation assay, n=8 wells. (E) Gene expression via qPCR of *ACTA2*, *ANXA3*, *CD55*, *CPE*, and *LOX,* normalization was performed relative to *GAPDH*. **** P<0.0001, *** P<0.001, ** P<0.01, ns P>0.05 by two-tailed unpaired t-test.